Available online at www.sciencedirect.com
SCIENCE DIRECT®
Journal of Sound and Vibration 271 (2004) 1133–1146
JOURNAL OF SOUND AND VIBRATION
www.elsevier.com/locate/jsvi

Letter to the Editor

Dynamic response analyses of vehicle and track coupled system on track transition of conventional high speed railway

Xiaoyan Lei*, Lijun Mao

Department of Civil Engineering, East China Jiaotong University, 330013 Nanchang, People's Republic of China

Received 10 January 2003; accepted 27 May 2003

1. Introduction

Transition regions are locations where a railway track exhibits abrupt changes in vertical stiffness [1]. They usually occur at the abutments of open deck bridges, where a concrete sleeper track changes to a wooden sleeper track, at the ends of a tunnel, at highway level crossings, at locations where rigid culverts are placed close to the bottom of the sleepers in a ballasted track, etc., shown in Fig. 1. Track transitions caused by a change of rail cross-section are rare and their effect is generally very small. Therefore, they will not be considered here.

Transition regions require frequent maintenance. When neglected, they will deteriorate at an accelerated rate. This may lead to pumping ballast, swinging or hanging sleepers, permanent rail deformations, worn track components, and loss of surface and gauge. These in turn may create a potential for a derailment.

A large quantity of abutments of open deck bridges, road crossings and tunnel ends exist in Chinese railway lines. For instance, the total length of the Beijing-Shanghai railway line is 1459 km and there are 1471 abutments of bridges and 490 road crossings on this line. In the past, the average speed of the trains in China usually was less than 80 km/h. The track transition problem is not serious in this situation. However, it has to be solved as the speed of trains in China is increased. The maximum train speed possible is 160 km/h according to Chinese railway regulation [2].

To clarify this problem, a dynamic computational model for the vehicle and track coupled system is developed by means of the finite element method. In numerical implementation, the vehicle and the track coupled system is divided into two parts, i.e., lower structure and upper structure. The vehicle as upper structure in the coupled system is a whole locomotive or carriage with two layers of springs and dampers in which vertical and pitch motion for the vehicle body and bogie are included. The lower structure in the coupled system is railway track where rails are considered as beams with finite length resting on a double layer continuous elastic foundation.

*Corresponding author. Tel.: +86-791-7046006; fax: +86-791-7046924.
E-mail address: leixy@ecjtu.jx.cn (X. Lei).

0022-460X/$ - see front matter
doi:10.1016/S0022-460X(03)00570-4

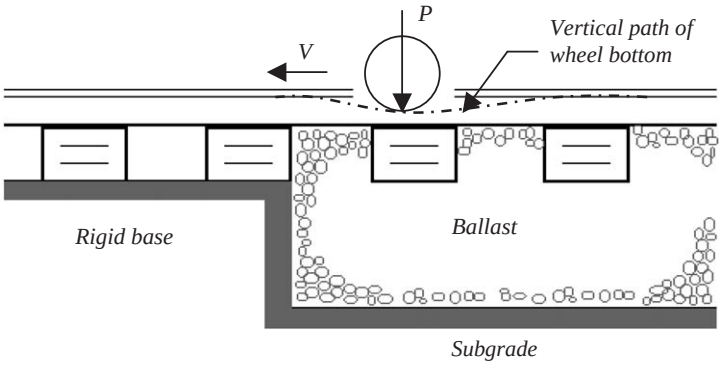

Fig. 1. Abutment of open deck bridge or tunnel ends in track transition.

The two parts are solved independently with an iterative scheme. Coupling the vehicle system and the railway track is realized through interaction forces between the wheels and the rail. Based on the model, dynamic response analyses of the vehicle and track coupled system at a track transition are then performed, where various train speeds and different settlements on track transitions are considered, and some conclusions are given.

2. Models for analysis of the vehicle and track coupled system

Studies [3–14] have been published on the vibration in a railway track under moving vehicles and different theories and models have been presented. In this paper, a more comprehensive dynamic analysis model for the vehicle and track coupled system will be developed.

Since the vehicle and the railway track are symmetrical about the centreline of the track and the longitudinal motion of the track has no effect on results, only half of the coupled system and only vertical vibration behavior are considered for the ease of calculation. The model for the analysis of dynamic responses of the vehicle and track coupled system at a track transition is shown in Fig. 2.

2.1. Dynamic equation of vehicle

The upper structure in the coupled system is a whole locomotive or carriage with two layers of springs and dampers in which vertical and pitch motion for both vehicle body and bogie are considered. The structure above the secondary suspension of the locomotive or the carriage is considered as a rigid body with mass and rotation inertia. In this case, the vehicle structure has ten degrees of freedom, i.e. seven vertical displacements and three pitch motions.

Defining a whole vehicle as a computational element, the nodal displacement vector and load vector for this element can be defined as

$$\{a\}_u = \{\, v_c \quad \varphi_c \quad v_{t1} \quad v_{t2} \quad \varphi_{t1} \quad \varphi_{t2} \quad v_{w1} \quad v_{w2} \quad v_{w3} \quad v_{w4} \,\}^{\mathrm{T}}, \tag{1}$$

$$\{Q\}_u = \{\, -M_c g \quad 0 \quad -M_t g \quad -M_t g \quad 0 \quad 0 \quad P_1 \quad P_2 \quad P_3 \quad P_4 \,\}^{\mathrm{T}}, \tag{2}$$

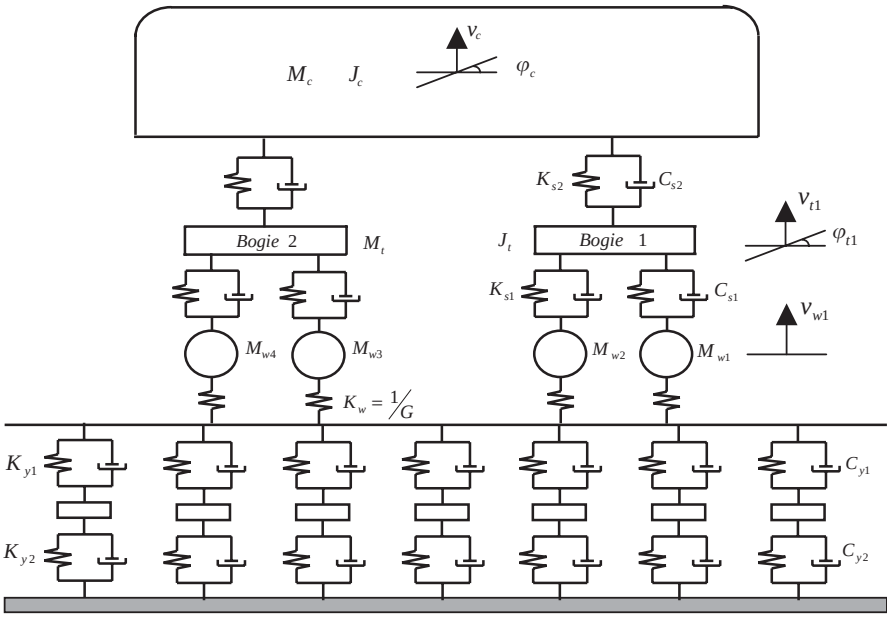

Fig. 2. Model for analysis of the vehicle and track coupled system on track transition.

where $P_i = -M_{wi}g + F_{wi}$, $M_{w1} = M_{w2} = M_{w3} = M_{w4}$, v_c and φ_c are the vertical displacement and pitch motion for the rigid body of the vehicle, v_{ti} and φ_{ti} are the vertical displacement and pitch motion for the ith bogie, M_{wi} is the mass of the ith wheel and F_{wi} is the interaction force resulting from the ith wheel of the vehicle contact with the rail.

The dynamic equation of the vehicle in the coupled system can be given as

$$[M]_u\{\ddot{a}\}_u + [C]_u\{\dot{a}\}_u + [K]_u\{a\}_u = \{Q\}_u, \tag{3}$$

where $[M]_u$, $[C]_u$ and $[K]_u$ are mass, damping and stiffness matrices for the upper structure. Explicit expressions for these matrices are given in Ref. [15].

2.2. Dynamic equation of railway track

The lower structure in the coupled system is the railway track where the rails are considered as beams of finite length resting on a double layer continuous elastic foundation. The finite element method is employed to establish the dynamic equation of the railway track, where rails as beams with transverse and bending deformation are discretized as two-dimensional beam elements and the rail between two neighboring sleepers is treated as one element. The masses of the sleepers are attached to the nodes of the beam elements as point masses. The masses of the ballast are simplified as point masses too and only vertical dynamic responses are considered. In order to reduce the bandwidth of the global stiffness matrix of the finite element equation and to simplify programming, a generalized beam element [16] for track structure is used here. In the generalized beam element, an additional vertical displacement v_i^* for the ballast mass is added to the normal 2D beam element, i.e. the element with two variables (v_i, θ_i) at each node is changed to one with

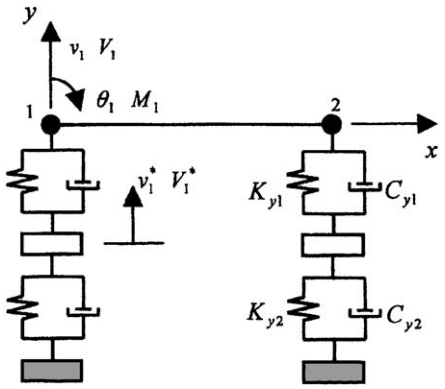

Fig. 3. Generalized beam element for track structure.

three variables (v_i, θ_i, v_i^*) per node, as shown in Fig. 3. The elastic and damping behavior of the rail fastenings and ballast as well as the roadbed in the vertical direction are represented by equivalent stiffness coefficients K_{y1}, K_{y2} and damping coefficients C_{y1}, C_{y2}. Hence, we can define the nodal displacement vector and nodal force vector for this generalized beam element as

$$\{a\}_l^e = \{\, v_1 \quad \theta_1 \quad v_1^* \quad v_2 \quad \theta_2 \quad v_2^* \,\}^{\mathrm{T}}, \tag{4}$$

$$\{Q\}_l^e = \{\, V_1 \quad M_1 \quad V_1^* \quad V_2 \quad M_2 \quad V_2^* \,\}^{\mathrm{T}}. \tag{5}$$

The stiffness matrix of the element can be expressed as

$$[K]_l^e = [K]_b^e + [K]_e^e = \begin{bmatrix} \frac{12EA}{l^3} & -\frac{6EI}{l^2} & 0 & -\frac{12EA}{l^3} & -\frac{6EI}{l^2} & 0 \\ & \frac{4EI}{l} & 0 & \frac{6EI}{l^2} & \frac{2EI}{l} & 0 \\ & & 0 & 0 & 0 & 0 \\ & & & \frac{12EI}{l^3} & \frac{6EI}{l^2} & 0 \\ & \text{Symm} & & & \frac{4EI}{l} & 0 \\ & & & & & 0 \end{bmatrix} + \begin{bmatrix} K_{y1} & 0 & -K_{y1} & 0 & 0 & 0 \\ & 0 & 0 & 0 & 0 & 0 \\ & & K_{y1}+K_{y2} & 0 & 0 & 0 \\ & & & K_{y1} & 0 & -K_{y1} \\ & & & & 0 & 0 \\ & & & & & K_{y1}+K_{y2} \end{bmatrix}, \tag{6}$$

where $[K]_b^e$ and $[K]_e^e$ are stiffness matrices resulting from the beam element and the elastic supports. E, A and I are the modulus of elasticity, cross-sectional area and moment of inertia for the rail and l is the length of the element.

The mass matrix of the element is

$$[M]_l^e = [M]_b^e + [M]_e^e = \frac{\rho A l}{420}\begin{bmatrix} 156 & -22l & 0 & 54 & 13l & 0 \\ & 4l^2 & 0 & -13l & -3l^2 & 0 \\ & & 0 & 0 & 0 & 0 \\ & & & 156 & 22l & 0 \\ & \text{Symm.} & & & 4l^2 & 0 \\ & & & & & 0 \end{bmatrix} + \begin{bmatrix} m_p & & & & & 0 \\ & 0 & & & & \\ & & m_b & & & \\ & & & m_p & & \\ & & & & 0 & \\ 0 & & & & & m_b \end{bmatrix}, \tag{7}$$

where $[M]_b^e$ and $[M]_e^e$ are mass matrices resulting from the beam element and sleeper and ballast masses. ρ is the density of the rail, m_p and m_b are half masses of the sleeper and the ballast between two sleepers, respectively.

The damping matrix of the element is usually expressed as

$$[C]_l^e = [C]_b^e + [C]_e^e = \alpha[M]_b^e + \beta[K]_b^e + [C]_e^e, \tag{8}$$

where

$$[C]_e^e = \begin{bmatrix} C_{y1} & 0 & -C_{y1} & 0 & 0 & 0 \\ & 0 & 0 & 0 & 0 & 0 \\ & & C_{y1}+C_{y2} & 0 & 0 & 0 \\ & & & C_{y1} & 0 & -C_{y1} \\ & \text{Symm.} & & & 0 & 0 \\ & & & & & C_{y1}+C_{y2} \end{bmatrix}, \tag{9}$$

where $[C]_b^e$ and $[C]_e^e$ are damping matrices resulting from the beam element and damping components. α and β are damping coefficients which depend upon the damping ratio and the natural frequency of the system. Such a damping is called proportional damping or vibration damping.

The equivalent nodal load vector for the generalized element in case of an intermediate force location, as shown in Fig. 4, can be expressed as

$$\{Q\}_l^e = \left\{ \frac{b^2(l+2a)P_y}{l^3} \quad -\frac{ab^2P_y}{l^2} \quad 0 \quad \frac{a^2(l+2b)P_y}{l^3} \quad \frac{ba^2P_y}{l^2} \quad 0 \right\}^{\mathrm{T}}. \tag{10}$$

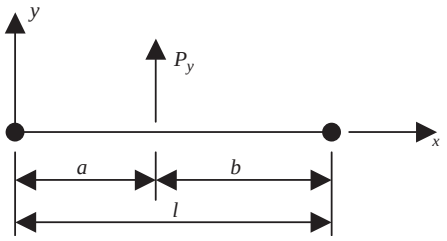

Fig. 4. Generalized beam element in case of intermediate forces.

The finite element dynamic equation for the railway track can be written as

$$[M]_l\{\ddot{a}\}_l + [C]_l\{\dot{a}\}_l + [K]_l\{a\}_l = \{Q\}_l, \tag{11}$$

where $[M]_l = \sum_e [M]_l^e$; $[C]_l = \sum_e [C]_l^e$; $[K]_l = \sum_e [K]_l^e$; $\{Q\}_l = \sum_e \{Q\}_l^e$.

These are the global mass, damping and stiffness matrices for the lower structure, which can be assembled by matrices of element mass, element damping and element stiffness.

3. Numerical algorithms

In the numerical implementation, we will divide the vehicle and track coupled system into two parts, lower structure and upper structure, and solve them independently with an iterative scheme [13,14,16,20,21]. Coupling the vehicle system and the railway track can be realized through interaction forces between wheels and rail. The track vertical profile irregularity will be considered in calculating the interaction forces with the conventional Hertz formula. One advantage is that we can easily solve the non-linear problem resulting from calculating interaction forces with the conventional Hertz formula shown as in Eq. (16) and the other advantage is that we can avoid the unsymmetrical dynamic equation for the whole coupled system.

3.1. Newmark integration method

In analyzing the dynamic responses of either the lower structure or the upper structure, the following dynamic equation needs to be solved by a numerical method

$$[M]\{\ddot{a}\} + [C]\{\dot{a}\} + [K]\{a\} = \{Q\}. \tag{12}$$

The Newmark integration method is an effective numerical technique [17], which is widely used in engineering practice. If solution ${}^t\{a\}, {}^t\{\dot{a}\}, {}^t\{\ddot{a}\}$ of Eq. (12) at time step (t) is known, the solution at time step ($t + \Delta t$) can be obtained by the following equation:

$$\begin{aligned}([K] + a_1[M] + a_2[C])^{t+\Delta t}\{a\} = {}& {}^{t+\Delta t}\{Q\} + [M](a_1{}^t\{a\} + a_3{}^t\{\dot{a}\} + a_4{}^t\{\ddot{a}\}) \\ & + [C](a_2{}^t\{a\} + a_5{}^t\{\dot{a}\} + a_6{}^t\{\ddot{a}\}),\end{aligned} \tag{13}$$

where $a_1 = 1/(\alpha\Delta t^2)$, $a_2 = \delta/(\alpha\Delta t)$, $a_3 = 1/(\alpha\Delta t)$, $a_4 = 1/(2\alpha) - 1$, $a_5 = \delta/\alpha - 1$, $a_6 = (\delta/(2\alpha) - 1)\Delta t$, α, δ are Newmark parameters. When $\alpha = 0.25$, $\delta = 0.5$, solution of the Newmark integration method is unconditionally stable [17].

3.2. Iteration scheme

1. *Initial computation*: In the first time step and first iteration, the interaction force vector ${}^{0}\{F\}$ should be assumed. The relative displacement between wheel and rail can be calculated by the conventional Hertz formula

$$y_i = GF_i^{2/3}, \tag{14}$$

where y_i and F_i are the relative displacement and interaction force between the (i)th wheel of the vehicle and the contacted rail, $G = 4.57R^{-0.149} \times 10^{-8}\,\mathrm{m/N^{2/3}}$ when the wheel tread is conic in shape and $G = 3.86R^{-0.115} \times 10^{-8}\,\mathrm{m/N^{2/3}}$ for the wheel of worn tread and R is the wheel radius [16].

If v_{xi}, the initial displacement of the rail at contact point with the (i)th wheel of the vehicle, is known the initial absolute displacement of the (i)th wheel v_{wi} can be calculated by

$$v_{wi} = y_i + v_{xi}, \tag{15}$$

where both v_{xi} and v_{wi} are defined as positive in the upward direction.

2. *Step by step procedure in time domain*: Assuming that in time step $(t + \Delta t)$, the (k)th iteration has been done, and vectors of the displacement, velocity and acceleration at time step (t) for lower and upper structures, ${}^{t}\{a\}_l, {}^{t}\{\dot{a}\}_l, {}^{t}\{\ddot{a}\}_l$ and ${}^{t}\{a\}_u, {}^{t}\{\dot{a}\}_u, {}^{t}\{\ddot{a}\}_u$, are obtained. Now let us consider the $(k+1)$th iteration. In the $(k+1)$th iteration of the time step $(t + \Delta t)$, dynamic equations for lower structure and upper structure will be solved by a stagger scheme.

Stage 1: From v_{wi} and v_{xi}, compute the interaction force vector ${}^{t+\Delta t}_{k+1}\{F\}_l$, in which

$$F_i = \begin{cases} \dfrac{1}{G^{3/2}}\left(\left|v_{wi} - (v_{xi} + \eta_i)\right|\right)^{3/2}, & v_{wi} - (v_{xi} + \eta_i) < 0, \\ 0, & v_{wi} - (v_{xi} + \eta_i) > 0, \end{cases} \tag{16}$$

where F_i is the component of the interaction force vector ${}^{t+\Delta t}_{k+1}\{F\}_l$, which is the force between the ith wheel and the contacted rail, and η_i is the irregularity of the track vertical profile at the contact point with ith wheel.

Applying ${}^{t+\Delta t}_{k+1}\{F\}_l$ to the lower structure as external forces, the solution for the track displacement ${}^{t+\Delta t}_{k+1}\{a\}_l$ can be obtained by solving dynamic equation (13). Then, the velocity ${}^{t+\Delta t}_{k+1}\{\dot{a}\}_l$ and acceleration ${}^{t+\Delta t}_{k+1}\{\ddot{a}\}_l$ at the $(k+1)$th iteration of the time step $(t + \Delta t)$ can be evaluated [17].

Stage 2: Check convergence of the solution.

Compute

$$\{\Delta a\}_l^k = {}^{t+\Delta t}_{k+1}\{a\}_l - {}^{t+\Delta t}_{k}\{a\}_l, \tag{17}$$

where ${}^{t+\Delta t}_{k+1}\{a\}_l$ and ${}^{t+\Delta t}_{k}\{a\}_l$ are displacement vectors of the lower structure at the current iteration and the previous iteration, respectively.

Now, define

$$\frac{\mathrm{Norm}\left(\{\Delta a\}_l^k\right)}{\mathrm{Norm}\left({}^{t+\Delta t}_{k}\{a\}_l\right)} \leqslant \varepsilon, \tag{18}$$

where ε is a specified tolerance.

If the convergence criterion (18) is not satisfied, go to Stage 3 and continue the computation. If it is satisfied, return to (2) step by step procedure in time domain and continue the computation in the next time step $(t + 2\Delta t)$.

Stage 3: Compute v_{xi} according to ${}^{t+\Delta t}_{k+1}\{a\}_l$ and calculate F_i by means of Eq. (16). Then ${}^{t+\Delta t}_{k+1}\{F\}_u$ can be obtained.

Stage 4: Applying ${}^{t+\Delta t}_{k+1}\{F\}_u$ to the upper structure as external forces, solution of the vehicle ${}^{t+\Delta t}_{k+1}\{a\}_u$ can be obtained by solving dynamic equation (13).

Stage 5: Compute v_{wi} according to ${}^{t+\Delta t}_{k+1}\{a\}_u$, go back to Stage 1 and continue the next iteration.

4. Verification

In order to test the effectiveness and the correctness of the model, the dynamic interaction forces between one wheel and the rail at a joint are analyzed, where 1.5 mm unevenness of level at the joint and different train speeds are considered. The parameters for the computation [18] are as follows:

C_{62} Chinese carriage with 210 kN axle load, $C_{s1} = 0$, $C_{s2} = 70$ kNs/m,
$K_{s1} = 1.0 \times 10^{15}$ kN/m, $K_{s2} = 5320$ kN/m,
rail cross-section area: $A = 0.7708 \times 10^{-2}$ m^2, moment of inertia: $I = 0.3203 \times 10^{-4}$ m^4,
modules of elasticity: $E = 2.1 \times 10^8$ kN/m^2, density of rail: $\rho = 7.83 \times 10^3$ kg/m^3,
elastic coefficients of the support: $K_{y1} = 6 \times 10^4$ kN/m, $K_{y2} = 8 \times 10^4$ kN/m,
damping coefficients of the support: $C_{y1} = 4.6 \times 10$ kN s/m, $C_{y2} = 9 \times 10$ kN s/m,
mass of the reinforced concrete sleeper: $m_p = 250$ kg, thickness of the ballast: $H = 35$ cm,
time step of the calculation: $\Delta t = 0.0004$ s.

The results are listed in Table 1 and compared with the measurement values [15]. The measurements were performed on site at the Beijing–Guangzhou railway line with the carriage train running both in step-up and step-down directions in the joints, where various unevenness of level at the joint and train speeds are chosen. Good agreement between the computations and the measurements can be seen from Table 1. The computational and experimental results also showed that travelling direction of the train has a small effect on the dynamic responses both for the track and for the vehicle.

5. Dynamic response analyses of vehicle and track coupled system on track transition

In the analyses of dynamic responses on the track transition, a TGV (French high speed train) locomotive is considered in this paper, as shown in Fig. 5. Parameters for the TGV locomotive are given in Table 2. In order to reduce the boundary effects of the rail, the total track length for the computation is 230.85 m (20 m for the transition region) with 405 generalized beam elements, which is more than 10 times the length of the vehicle. The running distance for the vehicle is 180 m. The track concerned is composed of 60 kg/m continuous welded long rails with reinforced concrete sleepers, 1760 pcs/km. The computational parameters for the railway track are the same as in the above test example.

Table 1
Maximum dynamic interaction forces between the wheel and the rail at a joint

Train speed (km/h)	Computation (kN)	Measurements (kN)	Relative error (%)
30	246	284	13.4
60	442	434	1.8
80	553	512	8.0

Table 2
Parameters for TGV locomotive

Parameter	Value	Parameter	Value
Axle load	170 kN	Radius of wheel	0.458 m
Rigid wheel base	3.0 m	Mass of the car	53500 kg
Mass of bogie	3260 kg	Mass of the wheel set	2000 kg
Stiffness of primary suspension	1.31×10^3 kN/m	Damping of primary suspension	30 kN s/m
Stiffness of secondary suspension	3.28×10^3 kN/m	Damping of secondary suspension	90 kN s/m

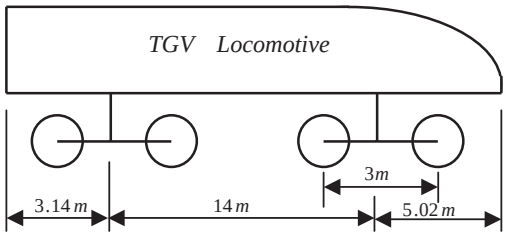

Fig. 5. Layout of TGV locomotive.

In order comprehensively to understand the dynamic responses of the coupled system on the track transition, the following parameter values are studied in the analyses:

No. 1: Train travelling at speeds of 60, 160, 250 and 300 km/h.
No. 2: Track in transition region with irregularity angles of $\alpha = 0$, 0.003, 0.006, 0.009, 0.012 rad, as defined in Fig. 6.
No. 3: Abutment or tunnel ends or road crossing with vertical roadbed stiffness coefficients of $10K_{y2}$ and $100K_{y2}$ where K_{y2} is vertical roadbed stiffness coefficient for conventional track, as shown in Fig. 7.

All computations are investigated with train travelling in the step-up direction in the transition region. The output results include the maximum vertical dynamic interaction force between the wheel and the rail P, maximum vertical acceleration of the vehicle body a_v and maximum vertical acceleration a_r for the rail. Results of the computations are shown in Tables 3–6 and in Figs. 8–10. From these computations, the following points can be obtained:

1. The vertical roadbed stiffness coefficient for the abutment of an open deck bridge or tunnel end or road crossing has little effect on vertical interaction force P between the

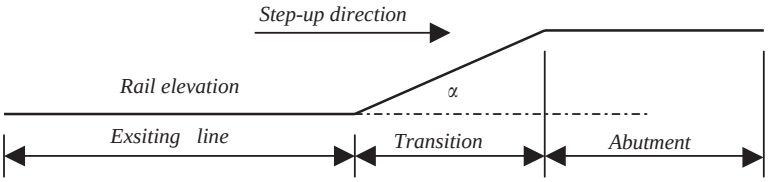

Fig. 6. Track transition with irregularity angle α.

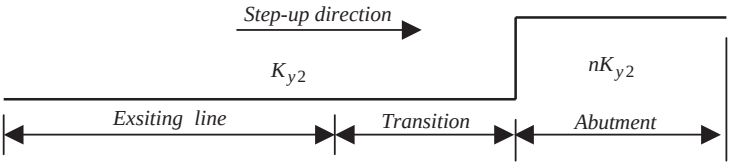

Fig. 7. Abutment or road crossing in track transition with vertical stiffness coefficient nK_{y2}.

wheel and the rail, the vertical acceleration of the rail a_r or the vertical acceleration of the vehicle a_v directly.

2. The irregularity angle of the track in the transition region has a significant influence on the vertical interaction force P, the vertical acceleration of the rail a_r and the vertical acceleration of the vehicle a_v, as shown in Tables 3–5. The presence of an irregularity angle of the track in the transition region means that settlement of the track vertical profile exists in this area. With the increase of the irregularity angle of the track the dynamic response for both vehicle and track increases greatly.
3. Figs. 8–10 present the maximum vertical interaction force between the wheel and the rail as well as maximum vertical accelerations of the rail and the vehicle for different speeds and irregularity angles. These show that, at constant train speed, the dynamic responses for the vehicle and the track increase as the irregularity angle of the track increases, and for a constant irregularity angle of the track the dynamic responses for the coupled system increase as the train speeds increase. In order to reduce the dynamic responses in a track transition, either the track irregularity has to be eliminated or the train speed has to be limited.
4. According to Ref. [2], the tolerance on the vertical acceleration of the vehicle for satisfying the requirement of riding index is 0.2 g. Based on the results of Table 6, the maximum irregularity angle of the track should be $\alpha \leqslant 0.006$ rad for a train speed of 160 km/h. Therefore if the allowable settlement in the transition region is 5 cm for a conventional high speed railway [2], the minimum length for the transition region should be $L = \Delta L/\alpha = 8.33$ m. Usually, $L \geqslant 10$ m is suggested for transition regions in practice.

The effective measures for improving the dynamic characteristics of the vehicle and the rail in a track transition are to strengthen the track structure and perform maintenance frequently, so that the irregularity can be controlled to a minimum range. Different measures have been presented and used by a number of railroad companies [1,15,19].

Table 3
Maximum interaction force P (kN) between wheel and rail at a speed of 250 km/h

Abutment stiffness	Irregularity angle α (rad)				
	0	0.003	0.006	0.009	0.012
$10K_{y2}$	123	277	467	671	885
$100K_{y2}$	125	276	468	672	885

Table 4
Maximum vertical acceleration of rail a_r (m/s^2) at a speed of 250 km/h

Abutment stiffness	Irregularity angle α (rad)				
	0	0.003	0.006	0.009	0.012
$10K_{y2}$	92.2	404	784	1200	1620
$100K_{y2}$	92.5	404	785	1200	1620

Table 5
Maximum vertical acceleration of the vehicle a_v (m/s^2) at a speed of 250 km/h

Abutment stiffness	Irregularity angle α (rad)				
	0	0.003	0.006	0.009	0.012
$10K_{y2}$	1.6	2.04	2.46	3.60	4.55
$100K_{y2}$	1.48	2.08	2.54	3.62	4.12

Table 6
Maximum vertical acceleration of the vehicle a_v (m/s^2) with roadbed stiffness K_{y2}

Irregularity angle α (rad)	Train speeds (km/h)			
	60	160	250	350
0	1.43	1.46	1.48	1.5
0.003	1.47	1.53	2.08	2.29
0.006	1.52	1.72	2.54	3.43
0.009	1.57	2.31	3.62	4.64
0.012	1.58	2.69	4.16	6.18

6. Conclusions

The amplitudes of vibration and the corresponding accelerations generated in the vehicle and the rail and the interaction forces between the vehicle and the rail in a track transition due to different irregularity angles of the track and at various train speeds have been analyzed here

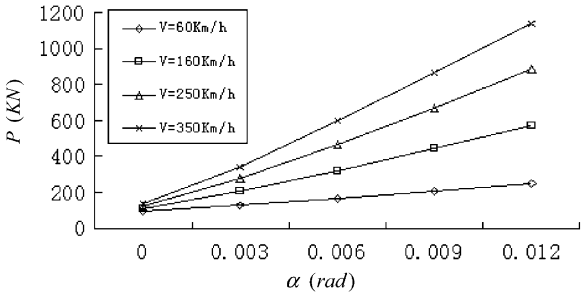

Fig. 8. Maximum vertical interaction force between vehicle and rail with different inclination angles.

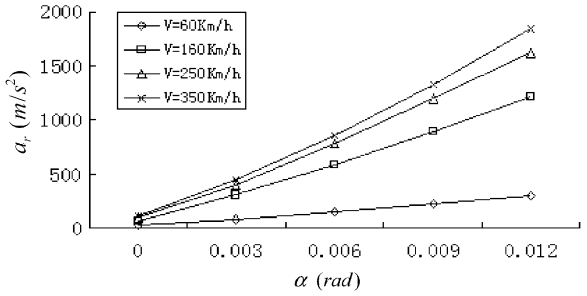

Fig. 9. Maximum vertical acceleration of rail with different inclination angles.

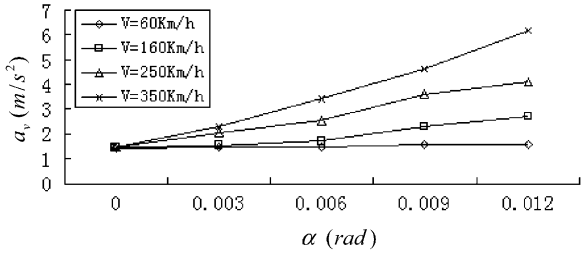

Fig. 10. Maximum vertical acceleration of vehicle body with different inclination angles.

numerically by a vehicle and track coupled computational model. The vehicle as upper structure in the coupled system is a whole locomotive or carriage with two layers of springs and dampers in which the vertical and pitch motion of the vehicle body and bogie are considered. The lower structure in the coupled system is the railway track where the rails are considered as beams of finite length resting on a double layer continuous elastic foundation. In the numerical implementation, the vehicle and track coupled system is divided into two parts, the lower structure and the upper structure, and solved independently with an iterative scheme. Coupling the vehicle system and the railway track is realized through interaction forces between the wheels and the rail. The advantages for analyzing the vehicle and track coupled system with an iterative

scheme are that we can easily solve the non-linear equation resulting from calculating interaction forces with the conventional Hertz formula and can avoid the unsymmetrical dynamic equation for the whole coupled system.

The computational results show that abrupt changes of vertical stiffness in a track transition do not lead to an increase of the dynamic interaction forces between the wheel and the rail directly, whereas the sudden permanent settlement of the track vertical profile in the track transition is the main source of the problem. As the final conclusion of this paper, the maximum irregularity angle of the track and the minimum length for the transition region are suggested for a Chinese conventional high speed railway.

Acknowledgements

The work reported herein was supported by Natural Science Foundation of China (50268001) and Natural Science Foundation of Jiangxi Province (0250034).

References

[1] A.D. Kerr, B.E. Moroney, Track transition problems and remedies, Bulletin 742, American Railway Engineering Association, 1996, pp. 267–297.
[2] Min Yaoxing, Raising train speed for existing railway, Chinese Railway Publication, 1997.
[3] M. Ishida, S. Miura, A. Kono, Track dynamic model and its analytical results, *RTRI Report* 11 (2) (1997) 19–26.
[4] M. Ishida, The past and future of track dynamic models, *RTRI Report* 14 (4) (2000) 1–6.
[5] Z. Cai, G.P. Raymond, Theoretical model for dynamic wheel/rail and track interaction, *Proceedings of the 10th International Wheel Set Congress*, Sydney, Australia, 1992, p. 9.
[6] H.H. Jenkins, J.E. Stephenson, G.A. Morland, D. Lyon, The effect of track and vehicle parameters on wheel/rail vertical dynamic forces, *Railway Engineering Journal* 3 (1974) 2–16.
[7] A.D. Kerr, Railroad engineering, Class Notes, University of Delaware, 1981.
[8] R.A. Clark, P.A. Dean, J.A. Elkins, S.G. Newton, An investigation into the dynamic effects of railway vehicles running on corrugated rails, *Journal of Mechanical Engineering Science* 24 (1982) 65–76.
[9] S.L. Grassie, R.W. Gregory, D. Harrison, K.L. Johnson, The dynamic response of railway track to high frequency vertical excitation, *Journal of Mechanical Engineering Science* 24 (1982) 77–90.
[10] M. Ishida, S. Miura, A. Kono, Track deforming characteristics and vehicle running characteristics due to the settlement of embankment behind the abutment of bridges, *RTRI Report* 12 (3) (1998) 41–46.
[11] J.C.O. Nielsen, Train/track Interaction: Coupling of Moving and Stationary Dynamic System, Dissertation, Chalmers University of Technology, Gotebory, Sweden, 1993.
[12] J. Kisilowski, K. Knothe, *Advanced Railway Vehicle System Dynamics*, Wydawnictwa Naukowo-Techniczne, Warsaw, 1991.
[13] W.M. Zhai, X. Sun, A detailed model for investigating vertical interactions between railway vehicle and track, *Vehicle System Dynamics* 23 (1994) 603–615.
[14] X.Y. Lei, Numerical analysis method of track structure, Chinese Railway Publication, 1998, pp. 69–72.
[15] X. Lei, N.-A. Noda, Analyses of dynamic response of vehicle and track coupled system with random irregularity of track vertical profile, *Journal of Sound and Vibration* 258 (1) (2002) 147–165.
[16] X.Y. Lei, New methods in railroad track mechanics and technology, *Journal of the Chinese Railway Society*, 2002.
[17] O.C. Zienkiewicz, *The Finite Element Method*, McGraw-Hill, New York, 1977.
[18] X.Y. Lei, Research on parameters of mechanical models for track structures of high speed railway, *Journal of the Eastern Asia Society for Transportation Studies* 3 (2) (1999) 29–37.

[19] Y. Sato, T. Usami, Y. Satoh, Development of ballast-Mat, *JNR Quarterly Reports* 15 (3) (1974) 125–130.
[20] F. Yang, A.F. Ghislain, An iterative solution method for dynamic response of bridge-vehicles systems, *Journal of Earthquake Engineering and Structural Dynamics* 25 (1996) 195–215.
[21] J.E. Snyder, D.N. Wormley, Dynamic interactions between vehicle and elevated, flexible randomly, irregular guide ways, *Journal of Dynamic Systems Measurement and Control* 99 (1977) 23–33.